MICROFLUIDICS ANALYSER FOR DISSOLVED ORGANIC CARBON

Duarte Nuno Mendonça Costa Moço
duarte.nuno.moco@ist.utl.pt

Instituto Superior Técnico, Lisboa, Portugal

Novembro de 2016

Abstract

Due to the vast multitude of reactions which dissolved organic carbon (DOC) is involved with in water systems, it is of great importance to obtain reliable results from the samples. One important aspect to consider is sample degradation occurring in the period between collecting the sample and analysis. To minimize this, a smaller, portable analyser capable of *in situ* analysis is required, which originates the call for a microfluidic analyser. This project studies the mesochannel geometry, inlet velocity and mixing efficiency relation to create a small compact microfluidic analyser. Simulations were carried out to understand aqueous solutions dynamics in mesochannels and predict the best mixing efficiency. Those simulated geometries were fabricated with Poly (methyl 2-methylpropenoate) (PMMA) structures, with the following cross-section dimensions: 1.0 mm wide and 0.5 mm deep.
Hopefully the results of this study may contribute to the miniaturization process of this analyser and many other similar projects.
Key-words: dissolved organic carbon, microfluidic simulation, fluid mixing, micromachining.

1.Introduction

Environmental scientists are increasingly emphasizing the geochemical and ecological roles of organic matter in aquatic ecosystems, since organic matter in aqueous systems often controls geochemical processes by acting as a proton donor or acceptor and as a pH buffer, by affecting the transport and degradation of pollutants, and by participating in mineral dissolution and precipitation reactions [1,2]. This organic matter is quantifiably divided between particulate organic carbon (POC), and DOC [3,4] which is best described, in terms of water content, as: the concentration of carbon remaining in a water sample after all particulate carbon has been removed by filtration with a pore size for the filter between 0,2 and 1,0 µm and all inorganic carbon has been removed by acidification and sparging. [3–7]

Given the importance of measuring DOC, a combined effort between INESC-MN and CESAM-UA, was done to develop a more reliable analyser

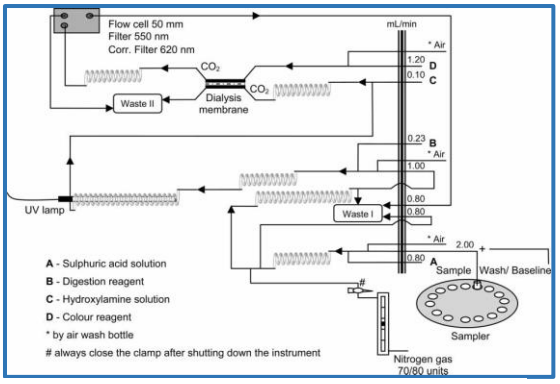

Figure 1: Flow diagram for dissolved organic carbon (DOC) analysis. [8]

to determine DOC, particularly one that could avert errors induced by sample degradation, which occurs between collecting that sample and analysing it. This thesis was born out of frequent analysis of the water samples from estuary of the river Vouga, located near the city of Aveiro, performed by the team in CESAM and their need for a smaller, portable device capable of shipboard analysis *in situ*.

This new microfluidic analyser will operate with the same underlying process of the commercially available SKALAR™ DOC analyser at the Aveiro University. The process, as described in Figure 1 [8], is based on the Wet Chemical Oxidation (WCO) technique for determining DOC. The sample is mixed with a sulphuric acid solution (Reagent A-Figure 1) to convert carbon from inorganic matter into carbon dioxide (CO_2) which is later sparged by bubbling with Nitrogen (N_2), after removal of gaseous phase (N_2 plus inorganic CO_2), the sample is mixed with a digestion reagent (Reagent B- Figure 1) is added to the solution, the mixture is them inserted in a third mixing coil, and following it, the mixture is irradiated in a digestion coil with a UV lamp (wavelength 185 nm) converting dissolved organic matter into CO_2. After organic matter oxidation, a hydroxylamine solution (Reagent C- Figure 1) is added to the sample. Afterwards, the mixture enters the dialyser composed of two overlapping channels separated by a semi-permeable membrane through which carbon dioxide can pass by diffusion. The sample flows through one of the channels, the CO_2 diffuses through the membrane into the other channel, where a weakly buffered phenolphthalein indicator (Reagent D- Figure 1) is flowing in counter current to the sample. DOC content in the sample is then determined by measuring colour intensity at 540 nm with a 650 nm thus measuring the discolouring of a phenolphthalein solution due to a pH change induced by the concentration of CO_2.

With the scope of miniaturising the analyser, a study was conducted to determine the relation between mesochannel geometries and inlet velocity with mixing efficiency.

2. COMSOL Multiphysics 5.0 Simulations

The mesochannels architecture were designed and simulated using COMSOL Multyphysics 5.0 to ascertain their mixing properties. The simulating conditions are based on the simulations described in Ref.[9] The models chosen for simulation were 'Laminar flow' for flow analysis and 'Transport of Diluted Species' for visualizing mixing. For simulations purposes all fluids were assumed to possess the same properties as liquid water at ambient temperature, using the specifications from the material library of the COMSOL Multiphysics 5.0. The analyser is expected to work at room temperature, so in this simulations temperature was set at 20ºC. To select inlet velocity, it was assumed that the flow in the microfluidic analyser should be as similar as possible to the current SKALAR™ analyser, as such the Reynolds number (Re) is assumed to be the same for both instances.

$$Re = \frac{\rho . u . D}{\mu} \quad (1)$$

With a temperature of 20ºC, water density (ρ) is 998.21 kg/m3 whereas dynamic viscosity (μ) was considered as 1.0016 mPa.s. The remaining flow properties in the SKALAR™ analyser are specified in Table 1.

Reynolds number, Re	28.20
Inner Diameter, D (m)	1.50×10^{-3}
Cross section area of the tube (m^2)	1.77×10^{-6}
Inlet velocity, u (m/s)	1.89×10^{-2}
Flow rate, Q (mL/min)	2,0
Dynamic viscosity at 20ºC, μ (Pa.s)	$1.00\ 10^{-3}$
Density at 20ºC, ρ (Kg/ m^3)	998.21

Table 1: Flow properties in the SKALAR™ analyser

The mesochannels, were designed with a rectangular cross section with 0.5 mm of height (h) and 1.0 mm of width (w). The hydraulic diameter, D_H, was calculated through the following equation:

$$D_H = \frac{4 \cdot Area}{Perimeter} \leftrightarrow D_{H\,rectangle} = \frac{4 \cdot h \cdot w}{2(h+w)} = \frac{2 \cdot h \cdot w}{(h+w)} \quad (2)$$

Following the calculation of the hydraulic diameter, inlet velocity and flow rate can be determined with Eq. (1) and is displayed in Table 2.

Reynolds number, Re	28.20
Hydraulic Diameter, D_H (m)	6.67×10^{-4}
Cross section area of the tube (m^2)	5.00×10^{-7}
Inlet velocity, u (m/s)	**4.24×10^{-2}**
Flow rate, Q (mL/min)	**1.27**
Dynamic viscosity at 20ºC, μ (Pa.s)	1.00×10^{-3}
Density at 20ºC, ρ (Kg/ m^3)	998.21

Table 2: Flow properties in the mesochannels

The simulation was performed with the same inlet velocities (for both inlets) of 4.24×10^{-2} m/s. The boundary conditions such as 'average velocity' were imposed to both the inlets and the

outlet was kept at atmospheric pressure. The channel walls were assigned to *no slip conditions*. On the other hand, 'concentration' was assigned to both inlets, *convective flux* was imposed at outlet and *no flux conditions* was assigned to walls. No specific material as selected in the diffusion to run the simulation, since the analyser will require to mix several aqueous solutions with various compounds, so for testing we only specified that the concentrations for the inlet 1 and 2 would be as 0 mol/m^3 and 100 mol/m^3, respectively. Therefore, if full mixing is achieved the overall concentration would be 50 mol/m^3.

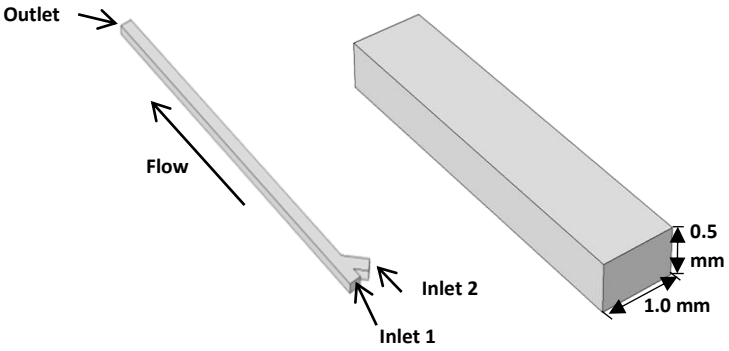

Figure 2: Geometry used for the mesochannels and the dimensions of channels

2.1 Generation-0 Models

A wide variety of geometries were simulated, varying parameters such as angle of joining of two channels, size and number of obstacles, to determine how they affect mixing.

The mesochannels have a cross section of 1mm width and 0.5 mm depth; the square pillars are designed to also have 0.5mm height. Inlet velocity of both inlets was set at 0.1 m/s and outlet relative pressure was set at 0 Pa. For this purpose, the simulations carried out for the Generation-0 mesochannels were divided in 4 types, per design: straight channels; square pillars (1-2) formation channels; square pillars (1-1) formation channels; and curved channels. (Figures 2 and 3)

2.1.1. Simulation of Straight channels

The straight mesochannel was tested to determine if a good level of mixing could be achieved with simple structures by mere diffusion and what effect the junction angle, formed by the interception of the two inlets, had on mixing. The junction angles tested were 180, 90 and 45 degrees formed by the two inlets. It revealed that some degree of mixing occurs but it is very inefficient, also the junction angle formed has very little impact in the degree of mixing, so later designs possess a 45 degree angle which allows a better organisation of the inlets, making it possible for the design to have all sample and reagents inlets in the same side. Figure 4 exemplifies the simulation results obtained from represents the simulation of transport diluted

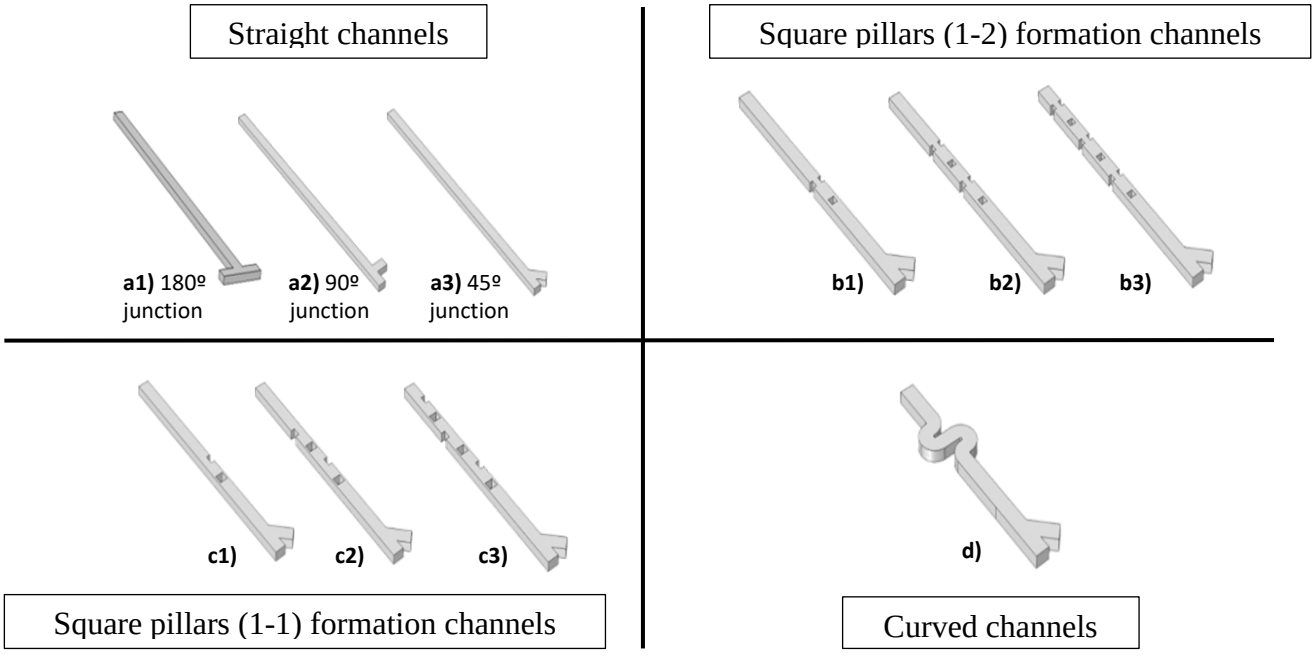

Figure 3: (a) Straight Mesochannels with 45 degree junction, 90 degree junction and 180 degree junction (1,2 and 3, respectively); (b) Straight Mesochannels with square pillars 3, 6 and 9 pillars (1,2 and 3, respectively); (c) Straight Mesochannels with square pillars 2, 4 and 6 pillars (1,2 and 3, respectively); (d) Curved Mesochannels.

species performed in all models, both Generation-0 and Generation-1.

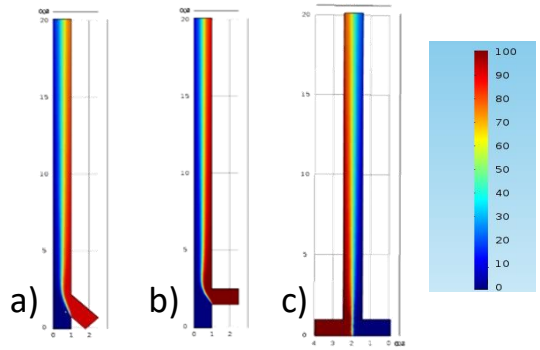

Figure 4: Concentration of the straight channels, a) with 45º, b) with 90º and c) with 180º angle between inlet. The mesochannels have 20 mm of length. Scale represents a colour code for the concentration gradient in mol/m^3. View of a XY plane crossing the middle of the mesochannel

2.1.2 Simulation of Square pillars (1-1) formation channels

This design was chosen to test if mixing could be easily reached with simple square shaped obstacles to disrupt fluid flow inside the mesochannels and create turbulence.

For the design, the straight section of the mesochannel is alternated between square obstacles in the center of the mesochannel and half a square pillar attached to the side (alternating between sides) of the mesochannel.

Simulations show that with bigger obstacles is possible to achieve better the mixing, with the 0.7 mm pillars showing the most promising results. However, during manufacture further described in chapter 3, it was revealed that tampering too much with the size of these obstacles poses some challenges, since thinner pillars can be easily broken off, even by the mill itself during mesong, and wider pillars may lead to obstructions that completely stop the flow.

2.1.3 Simulation of Square pillars (1-2) formation channels

Following a design similar to the one employed on the previous simulations, with extra obstacles to increase fluid flow disruption in an attempt to further increase mixing.

For the design, the straight section of the mesochannel is alternated between square obstacles in the centre and half a square pillar attached to both sides of the mesochannel.

Alike the (1-1) square pillars formation mesochannels, mixing increases with greater size of the obstacles and with greater number of them, but also has the same challenges with changing the size of the pillars. Although, since (1-2) formation possesses more obstacles than the (1-1) formation, mixing is better on the former mesochannels as expected.

2.1.4 Simulation of Curved channels

Curved microchannel was chosen for their compactness in the design and to study the effect on mixing due to their non-uniform shapes.

Simulations suggest that mixing is better with wider curves, however with narrower curves, despite having a slightly worst mixing, the length of the structure is significantly reduced. Since one of the objectives, is to make a structure as small as possible, the overall length of the structure will also have to be equated to optimize mixing with the shortest length possible.

2.1.5 Simulation of different inlet velocities in different inlets

This simulation was designed to test the effect of different inlet velocities would have on mixing, for that purpose three straight mesochannels were tested: one straight channel with the same inlet velocity; another with the inlet on the left with double the velocity of the right; and another channel with the double inlet velocity on the right than on the left.

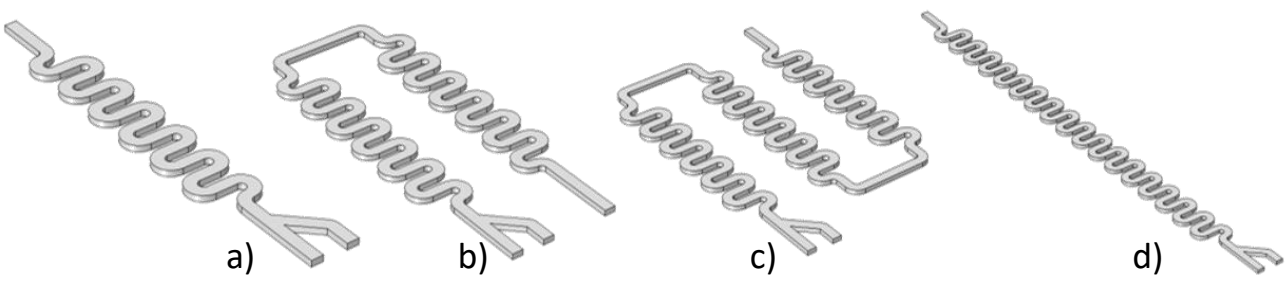

Figure 5: Models for the Generation-1 mesochannels: a) short curved mesochannel (ShM); b) U-shaped curved mesochannel (UM); c) S-shaped curved mesochannel (SM); d) long curved mesochannel (LM). Cross section in all mesochannels is 0.5 mm high and 1.0 mm wide

In the simulations, different velocities in different inlets do not produce any significant change in the mixing, which means that if the flowrate of two solutions are different it is, fairly, safe to assume to have similar mixing requirements as if the flowrates were the same.

2.2 Generation-1 Models

The first experimental testing revealed that of the Generation-0 mesochnnels, only the curved mesochannels were capable of being manufactured into working conditions using the procedure described in chapter 2, but the channel was either too short or had too little flow disruption to produce any significant mixing. As such. longer and more complex curved mesochannels were designed, simulated and then tested.

The new mesochannels were designed using AutoCAD 2016, by replicating the same curve several times and arranging the resulting structure into: a short curved channel (ShM), a U-shaped curved channel (UM), a S-shaped curved channel (SM) and a longer curved channel (LM). (Figure 5).

These designs were later uploaded into COMSOL Multiphysics 5.0 in the geometry section and then converted into 3D models by extruding height of 0.5 mm, and simulations were carried out as described in Chapter 3, with various inlet velocities, to determine if mixing can be achieved with slower velocities.

2.2.1 Simulation of Short Curved Mesochannels (ShM)

The Short Mesochannels (ShM) are the simplest design for stacked curved mesochannels, and simulations show that complete mixing is estimated to happen somewhere between the fourth and the seventh U-turn, depending on the inlet velocity. If the experimental testing corroborates these simulations, or the full mixing onset occurs, for the specified inlet velocities, within the length of the ShM, there will be no need for more complex or longer channels, with sole exception if the process occurring in these mesochannels require a greater residence time.

2.2.2 Simulation of U-shaped Curved Mesochannels (UM)

U-shaped Curved Mesochannels (UM), were designed with two objectives in mind: to increase the length and complexity of the ShM, in the event, that the full mixing does not occur within the length of the ShM, also this design offers the possibility of arranging the reagent inlets to be on the same side and close to each other, which translates in a simpler, smaller and closely packed structure for the entire chemical unit. Because of the similar design of the ShM, the simulations also suggest the same interval of to achieve full mixing is presented on the simulations of ShM, which means that full mixing is estimated to occur in between the fourth and the seventh U-turn.

2.2.3 Simulation of S-shaped Curved Mesochannels (SM)

With even greater length and complexity than the UM, the S-shaped Curved Mesochannels (SM) were designed with the concern that mixing may not occur within the length of the previous mesochannels for the chosen inlet velocities. Alike the previous mesochannels, full mixing is estimated to occur somewhere between the fourth and the seventh U-turn.

2.2.4 Simulation of Long Curved Mesochannels (LM)

Long Curved Mesochannels (LM) were designed out of the same concern behind the SM, and allows the possibility of determining the full mixing onset of a structure with a similar design as the ShM. Alike the previous mesochannels, full mixing is estimated to occur somewhere between the fourth and the seventh U-turn.

3. Methodology

The methodology behind the study begins by attempting to replicate mixing with smaller channels, since most of the process of determining DOC revolves around subjecting the sample to several reagents to convert inorganic impurities into CO_2 for immediate removal and converting organic matter into CO_2, these reactions will require an efficient mixing to achieve good conversion.

To better understand mixing to achieve the best results, mixing is simulated in several mesochannels with different designs, as described throughout chapter 3, and the most efficient designs are selected for experimental testing. This testing involves creating structures of Poly (methyl 2-methylpropenoate), more commonly known as Poly(methyl methacrylate) (PMMA) of the selected mesochannels and pumping coloured MilliQ water into the aforementioned mesochannels.

As such the production by converting the design with the most promising simulations into schematics using *AutoCAD 2016*, the selected

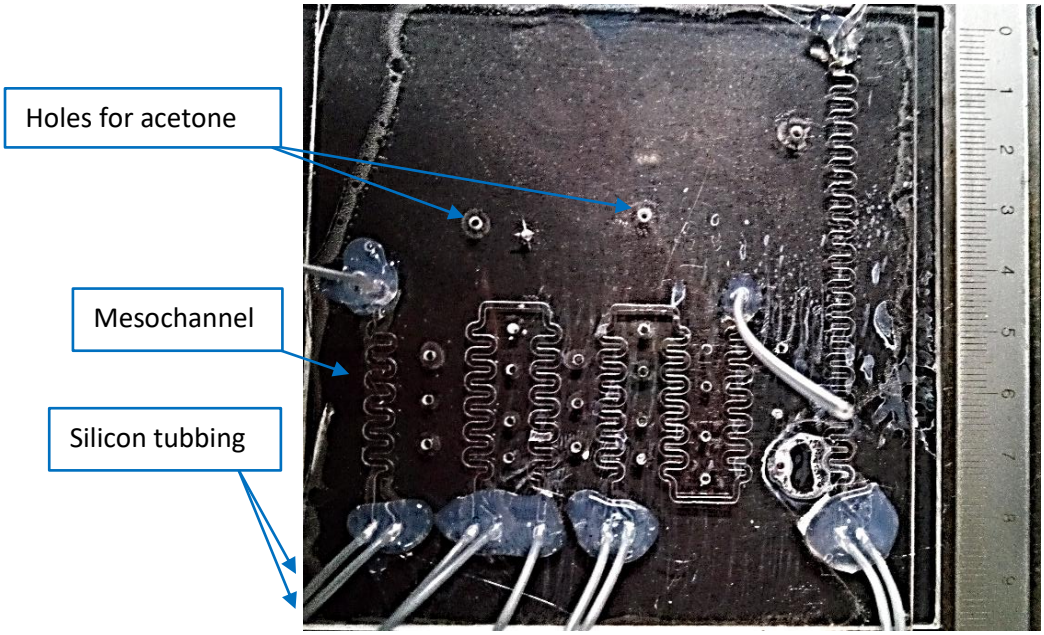

Figure 6: Top view of the PMMA structures used in the experimental tests, with silicone tubbing already attached to the proper holes in the PMMA. Caliber as reference on the left for scale.

designs of the structures was created with the white lines representing the mesochannels and the green lines representing the holes where the silicone tubbing introduced, to make the inlets and outlets.

These schematics are later milled using a 1.0 mm mill and drilled with a 1.5 mm drill into a piece of PMMA using a Milling Machine , for that the toothpaths were created using a *DESKAM 2000*.

After milling and drilling both pieces of PMMA, are fused together using acetone, for that purpose, it is required to drill a few extra holes for pouring acetone between the PMMA slabs and seal the mesochannels properly, to avoid leaking from one channel to another or the fluid taking "shortcuts" instead of following the desired path: this extra holes. Silicon tubbing (1,27 mm outer diameter) is then inserted in the holes for the inlets and outlets, then stanched with silicon sealant. (Figure 6)

4. Results and Discussion

The scope of these tests is to ascertain if mixing can be achieved in these mesochannels and test the effect of inlet velocity on the mixing. For that different flowrates were tested: 0,5 mL/min, 1,0 mL/min, 1,27 mL/min, 1,5mL/min and 2,0 mL/min.

Unfortunately, when assembling the PMMA structures often excess acetone poured into the mesochannels, fusing them shut, which left them in non-working condition. And despite several tries in assembling the PMMA structure correctly, the U-shaped mesochannel was never operational and could not be tested with, however data collected from the other mesochannels, make up for this mishap.

Nonetheless, after visual analysis of the photos taken during experimental testing and further analysis using ImageJ program through the analyse option "RGB profile", which decomposes

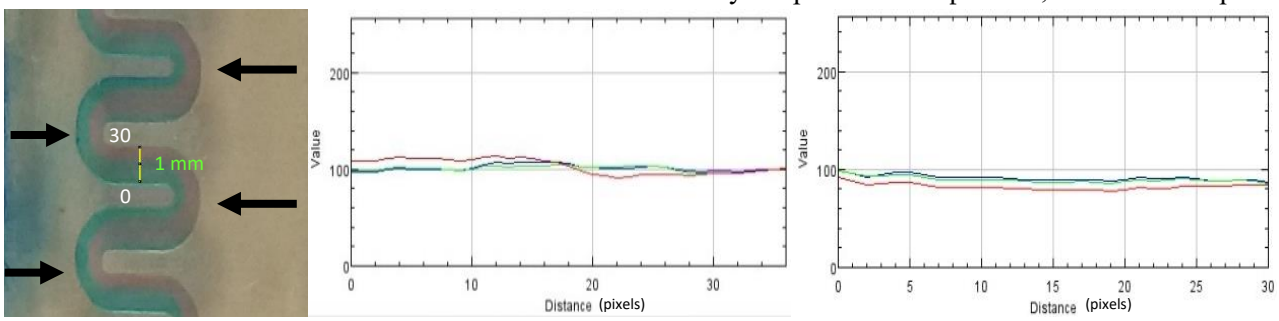

Figure 7: On the left, a representation of a cross section selected for analysis in ImageJ, also the 5 black arrows represent U-turn counting. In the middle, an RGB profile of a cross section, with the red showing a greater intensity in the first half of the cross section, and greater intensity of blue on the second half, suggesting incomplete mixing. On the right, colour intensity seems uniform without alternating the colour of greater intensity, suggesting complete mixing. In the graphs, "Distance" is measured in pixels, and "Value" represents colour intensity which is a dimensionless measure.

the colour of the pixels from a pre-selected line into three colours, Red, Blue and Green, and measures their intensity. The criteria used to determine mixing is by measuring the colour intensity in the cross-section of the mesochannel, if the blue and the red lines do not change positions relatively to each other, then mixing is achieved. Then the number of U-turns before full mixing are counted and recorded on Table 3, in this thesis, U-turns are considered all curves that turn the direction of the flow by 180 degrees.

Flow rates (mL/min)	*SM (36 turns)*	*LM (34 turns)*
0,50	N.M.	N.M.
1,00	N.M.	N.M.
1,27	36	N.M.
1,50	35	N.M.
2,00	31	34
3,00	24	26
4,00	23	24
5,00	22	21

Table 1: Number of U turns required to achieve full mixing in each channel (total number of U turns in the mesochannel in parenthesis). No mixing is represented by N.M.

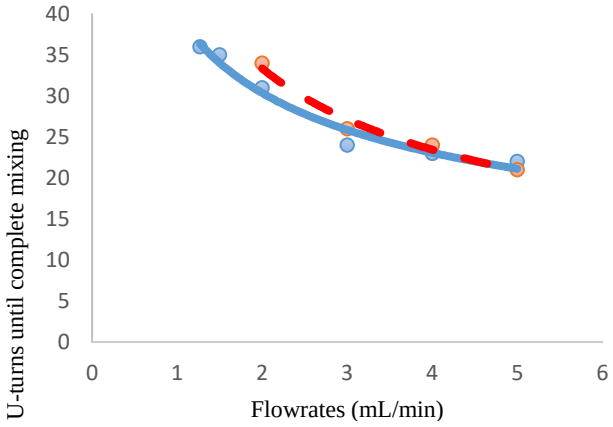

Figure 8 Representation of the full mixing onset on the SMs (with a solid line) and the LMs (with a dashed line) in a graph of Flowrate (mL/min) vs U-turns until complete mixing

During testing, as opposed to what the simulations suggested, ShM never showed full mixing, suggesting they required an even higher inlet velocity. As for the remainder working mesochannels, as it is shown in Table 3 and Figure 8, contrary to the simulation results for the flowrates from 0.50 mL/min to 2.00 mL/min, mixing did not occur between the 4th and 7th U-turn, where, in fact, only occurs on the longest mesochannels (SM and LM) with a minimum of 31 U-turns, and even then, the designed mesochannels were not long enough to achieve mixing with all the simulated flowrates. Because of this, there was not enough data to draw any valid conclusion, so, more tests were carried out with higher flowrates: 3.00 mL/min; 4.00 mL/min; and 5.00 mL/min.

With the results from extra inlet velocities, it can be concluded from the results that, with greater inlet velocities, mixing occurs earlier in the same structure, which means that the greater the velocity, the greater the mixing and shorter is the required structure.

5. Conclusion

From the obtained simulations and tests, one can see that mixing can be achieved in the proposed mesochannels, however there is a big discrepancy between the inlet velocities at which full mixing occurs. Determining the required length necessary for full mixing to occur is an important requirement to conjugate the length of the mesochannel with inlet velocity to optimize residence time.

This residence time is a key parameter to consider in building these mesochannels, since several reactions take place throughout the process and in the dialyser section, the diffusion of CO_2 through the Teflon membrane requires time. Having that in mind, this study suggests that it is possible to produce a closely packed mesochannel where both inlet velocity and size of the mesochannel can be adjusted to achieve full mixing with a specific residence time, without either creating a mesochannel too long or using too low of inlet velocities. To further test this hypothesis, this project would require more time and more complex PMMA structures, which are proving quite difficult to obtain since the Milling Machine is currently out of order.

On a side note, results also show that the S-shaped mesochannel provides better mixing, since it possesses the lowest full mixing onset, in addition, it is the only mesochannel among the designed that allows mixing with the same flow regime as the original analyser (flowrate 1.27 mL/min).

Development of this analyser has yet to reach the testing stage of proof of concept, several variables are yet to be tuned to optimize the device, however, there are already designs for the first mesochannel for the chemical unit to be tested in the proof of concept stage, once it is possible to reproduce it in a PMMA.

In summary, this thesis set out to create a smaller device for analysing DOC, but due to the time limitation given to this project, the thesis could only cover one of the four units that compose the SKALAR™ analyser, whose procedure the thesis attempted to emulate: the chemical unit. However given the outcome presented in the results, it can be

concluded is possible to reduce the size of the chemical unit, using the S-shaped curved mesochannel, which showed the best mixing efficiency, and adjusting both inlet velocity and length of mesochannels. These adjustments will be performed in greater depth on the "proof of concept" stage, which preparations are currently underway.

6. Bibliography

[1] Weishaar J, Aiken G, Bergamaschi B, Fram M, Fujii R, Mopper K. Evaluation of specific ultra-violet absorbance as an indicator of the chemical content of dissolved organic carbon. Environ Sci Technol. 2003;37(20):4702–8.

[2] Giancoli Barreto SR, Nozaki J, Barreto WJ. Origin of Dissolved Organic Carbon Studied by UV-vis Spectroscopy. Acta Hydrochim Hydrobiol 2003;31:513–8

[3] Monica Z. Bruckner, Montana State University B. Measuing Dissolved and Particulate Organic Carbon (DOC and POC) [Internet]. Available from: http://serc.carleton.edu/microbelife/research_methods/biogeochemical/organic_carbon.html

[4] of Saskatchewan G. Dissolved Organic Carbon (DOC) [Internet]. Government of Saskatchewan. 2009 [cited 2016 Oct 25]. Available from: http://www.saskh2o.ca/PDF-WaterCommittee/DissolvedOrganicCarbon.pdf

[5] Determination of dissolved organic carbon and total dissolved nitrogen in sea water [Internet]. 2007. p. 7. Available from: http://www.jodc.go.jp/geotraces/docs/PICESReport34_DOC_DON.pdf

[6] Benner R, Von Bodungen B, Farrington J, Hedges JI, Lee C, Mantoura F, et al. Measurement of dissolved organic carbon and nitrogen in natural waters: Workshop report. Mar Chem. 1993;41(1–3):5–10.

[7] Rene P. Schwarzenbach, Philip M. Gschwend DMI. Environmental Organic Chemistry. Second edition. Wiley Interscience A John Wiley & Sons, INC., Publication;

[8] Lopes CB, Abreu S, Válega M, Duarte RMBO, Pereira ME, Duarte a. C. The Assembling and Application of an Automated Segmented Flow Analyzer for the Determination of Dissolved Organic Carbon Based on UV-Persulphate Oxidation. Anal Lett. 2007;39(9):1979–92.

[9] Das SS, Patawari BK, Patowari PK, Halder S. Computational Analysis for Mixing of Fluids Flowing through Micro- Channels of Different Geometries. 2014